Journal of Chromatography A, 1218 (2011) 711–720

Contents lists available at ScienceDirect

Journal of Chromatography A

journal homepage: www.elsevier.com/locate/chroma

A density functional approach to retention in chromatography with chemically bonded phases

M. Borówko*, S. Sokołowski, T. Staszewski

Department for the Modeling of Physico-Chemical Processes, Maria Curie-Skłodowska University, 20031 Lublin, Poland

ARTICLE INFO

Article history:
Received 4 August 2010
Received in revised form 6 December 2010
Accepted 7 December 2010
Available online 15 December 2010

Keywords:
Density functional theory
Theory of chromatography
Bonded phases
Reversed liquid chromatography

ABSTRACT

A density functional approach to the retention in a chromatography with chemically bonded phases is developed. The bonded phase is treated as brush built of grafted polymers. The chain molecules are modelled as freely jointed spheres. Segments of all components interact with the surface via the hard wall potential whereas interactions between the segments are described by Lennard–Jones (12-6) potential. The structure of the bonded phase is investigated. The distribution of different solutes in the stationary phases is determined. An influence of the following parameters on the retention is analyzed: the grafting density, the grafted chains length, the strength of molecular interactions, the solute sizes, temperature. The theoretical predictions are consisted with numerous experimental results.

1. Introduction

Reversed-phase liquid chromatography is a method of choice for analytical separation of low molecular weight samples and the goal of numerous investigations has been to improve the selectivity and efficiency of the chromatographic separations. The important step towards optimization of the process is understanding the mechanism at the molecular level. The mechanism of the retention has been a matter of debate in the literature. One of the major and long-standing problems is whether solute molecules are retained by a partitioning or by an adsorption-like process. In the "partitioning" model the solute is fully embedded within the bonded phase and is surrounded almost exclusively with polymer segments. According to the "adsorption" model solute molecules adsorb onto the surface of the polymer film. In this case the solute molecules are in contact with the chain segments but are not fully embedded. However, recent theoretical and experimental investigations show that a real picture of the retention is much more complicated [1–3].

In the simplest model the stationary phase is treated as an amorphous fluid medium resembling the bulk polymer phase [4]. The retention is described as due to partitioning between two liquid phases or adsorption on modified surfaces. However, the grafted chains are constrained by the interface and cannot explore all possible conformations. The interfacial constraints cause that the grafted chains exhibit partial alignment of the chain normal to the surface. In other words, the grafted chains are more ordered than chains in the bulk phase. Several theoretical approaches to the solute retention in such systems were based on the lattice models of bonded phases and solutions [1,5–8]. The effects of chains organization in the stationary phase have been approximately taken into account in the Martire and Boehm theory [5]. Their approach neglects the variation of chain configurations with distance from the surface. They have assumed a uniform composition and density in the bonded phase. In that model the first segment is anchored at the solid surface, while the last segment is fixed in the layer adjacent to the mobile phase. This theory overestimates the ordering in the stationary phase.

More realistic model was introduced by Dill and coworkers [1,6]. Their theory predicts that the ordering of the bonded phase varies with a distance normal to the surface but the segment density profile is prefixed. The distribution of solute molecules in the stationary phase is found from thermodynamics. Dill and coworkers [1,6] assumed that solvent is absent in the bonded phase. Both these theories confirm a strong correlation between liquid/liquid partitioning and retention in reversed phase liquid chromatography. Fleer et al. [9] presented the general method to describe various interfacial systems involving polymers. The main idea behind their method is that the description of an inhomogeneous system of many interacting molecules is reduced to the problem of determining the statistical weight of chain conformations in an external potential field. They considered two conjugated functions, the density profiles and the potential profiles. In the self-consistent approach there are rules governing

* Corresponding author. Tel.: +48 815242251.
E-mail address: borowko@hektor.umcs.lublin.pl (M. Borówko).

0021-9673/$ – see front matter © 2010 Elsevier B.V. All rights reserved.
doi:10.1016/j.chroma.2010.12.029

how to obtain density profiles from the potentials and inversely. The self-consistent solution is achieved when these conjugated profiles becomes consistent each other. This theory was applied to study of the retention process in the reversed-phase liquid chromatography [7,8]. In this model all the components, including grafted chains, can adjust their densities to local conditions. Both solutes and solvents are assumed to be flexible oligomers.

The lattice-off models of bonded phases have been mainly used to study their structure [10]. One can distinguish several groups of theoretical approaches to the description of the systems involving polymer brushes, namely, phenomenological treatments [11,12], classical self-consistent field theory [13–16], single-chain mean-field method [17–19] and density functional theory [20–30]. Adsorption on the polymer brushes was relatively less investigated [29,30].

Numerous computer simulations have supplemented theoretical studies. Molecular dynamic simulations were performed for the systems without explicitly involved solvents [31–34], as well as for the systems containing water/methanol or water/acetonitrile mixture as the mobile phase [35–37]. The important series of articles devoted to Monte Carlo simulations of the retention has been recently published by Rafferty et al. [38–41]. They have presented the results obtained for the quite realistic models of the selected chromatographic systems. Their methodology makes possible the systematic study an influence of different parameters on the structure of the stationary phase and the solute retention.

The nature of chemically bonded phase considerably affects chromatographic separation. Therefore, structural and dynamic properties of alkyl stationary phases are intensively investigated using various spectroscopic techniques, including Raman [42–47], nuclear magnetic resonance [48–50], fluorescence [51,52], sum-frequency generation [53] spectroscopes and small angle neutron scattering [54].

In this work we propose density functional approach to the retention in chromatographic systems with chemically bonded phases. We extend the approach proposed in our previous papers [29,30]. We consider here sorption of a mixture of short linear chains on polymer brushes. We demonstrate that the proposed theory allows one to predict the salient features of the retention. The paper is arranged as follows. In the next section we introduce the model, discuss its limitations and describe briefly the theory. The results are presented and discussed in Section 3. Finally, we summarize the conclusions and show perspectives of future investigations. The computational method is described in Appendix A.

2. Theory

2.1. General formulation

We consider a two-component mixture of short linear chains in contact with a modified substrate. The surface is covered by chemically bonded phase, i.e., by the film of preadsorbed polymer molecules (labelled as "1" in what follows). We treat the system as a ternary mixture of polymeric chains, where the components $k = 2$ and 3 are solutes. All the polymers are represented by tangentially jointed spherical bead chains. The chain connectivity is enforced by the bonding potential between nearest-neighbor segments V_B, given by [23]:

$$\exp[-\beta V_B(\mathbf{R}_k)] = \prod_{i=1}^{M_k-1} \delta\frac{(|\mathbf{r}_{i+1} - \mathbf{r}_i| - \sigma^{(k)})}{4\pi(\sigma^{(k)})^2}, \quad (1)$$

where $\mathbf{R}_k \equiv (\mathbf{r}_1, \mathbf{r}_2, \cdots, \mathbf{r}_{M_k})$ is a vector specifying segment positions for the kth component, $\sigma^{(k)}$ and M_k are, respectively, the segment diameter and the number of segments for the kth component; $\beta^{-1} = k_BT$ stands for the Boltzmann constant multiplied by the absolute temperature.

Each polymer molecule of the chemically bonded phase contains one surface-binding segment located at its end (indexed as "1") that interacts with the wall via the potential:

$$\exp[-\beta v_{s1}(z)] = C\delta\left(z - \frac{\sigma^{(1)}}{2}\right), \quad (2)$$

where z is a distance from the surface, $\delta(z - \sigma^{(1)}/2)$ is the Dirac function and C is a constant. This potential implies that the surface-binding segments lie always at the distance $z = \sigma^{(1)}/2$ from the surface. The remaining segments of the grafted molecules ($j = 2, 3, \ldots, M_1$) are "neutral" with respect to the surface.

The hard-wall potentials are assumed for the interactions between the wall and "neutral" segments of the chemically bonded phase and for the interactions between segments of both components of the adsorbed mixture and the substrate:

$$v^{(k)}(z) = \begin{cases} \infty & z \le \sigma^{(k)}/2 \\ 0 & \text{otherwise} \end{cases}. \quad (3)$$

We assume the Lennard–Jones type interactions between all segments. Because of computational reasons we split these interactions into the repulsive (reference) and attractive (perturbation) parts according to the Weeks–Chandler–Anderson scheme [55]:

$$u^{(kl)}(r) = u^{(kl)}_{rep}(r) + u^{(kl)}_{att}(r). \quad (4)$$

The repulsive term is approximated by the hard-sphere potential

$$u^{(kl)}_{hs}(r) = \begin{cases} \infty & r \le \sigma^{(kl)} \\ 0 & \text{otherwise} \end{cases}. \quad (5)$$

where $r = |r_{ij}| = |r_i - r_j|$ is the center-to-center distance between spherical segments "i" and "j", where $\sigma^{(kl)} = 0.5(\sigma^{(k)} + \sigma^{(l)})$, k, $l = 1$, 2, 3.

The attractive part is given by

$$u^{(ij)}_{att}(r) = \begin{cases} -\varepsilon^{(kl)} & r < 2^{1/6}\sigma^{(kl)} \\ u^{(kl)}_{LJ}(r) & r \ge 2^{1/6}\sigma^{(kl)} \end{cases}, \quad (6)$$

where $u^{(kl)}_{LJ}(r)$ is the Lennard–Jones potential:

$$u^{(kl)}_{LJ}(r) = 4\bar{\varepsilon}^{(kl)}\left[\left(\frac{\sigma^{(kl)}}{r}\right)^{12} - \left(\frac{\sigma^{(kl)}}{r}\right)^{6}\right], \quad (7)$$

and where $\bar{\varepsilon}^{(kl)}$ is the Lennard-Jones energy parameter. In the work we use the energy parameters $\varepsilon^{(kl)}$ expressed in units of thermal energy k_BT, namely, we assume that $\varepsilon^{(kl)} = \bar{\varepsilon}^{(kl)}/k_BT$. We take the diameter of the grafted chains $\sigma^{(1)}$ as the unit of the length.

We define the segment density as $\rho^{(k)}_s = M_k\rho^{(k)}$, where $\rho^{(k)} = N_k/V$ is the number density (N_k is a number of molecules of the kth component, V is a volume). The segment density is a sum of densities of individual segments $\rho^{(k)}_{s,i}$:

$$\rho^{(k)}_s(r) = \sum_{i=1}^{M_k}\rho^{(k)}_{s,i}(r). \quad (8)$$

We assume that the grafting density $\rho_1 = N_1/A$ (where N_1 is a number of grafted chains and A denotes the surface area) is fixed. This means that the density of the first segment near the surface also remains fixed $\rho^{(1)}_{s,1}(\sigma^{(1)}/2) = const$. In real systems the maximum bonded phase density is roughly 4 μmol/m^2 (or 41.5 Å^2/chain). This corresponds to the grafting density $\rho_1 \approx 0.36$ (with $\sigma^{(1)} = \sigma_{CH_2} \approx 0.9$ Å) in our model.

The considered fluid is in equilibrium with the reservoir containing only molecules of solutes, $S = k = 2, 3$, where the bulk densities (bulk segment densities) are equal $\rho_b^{(k)}$ ($\rho_{bs}^{(k)}$). The chemical potentials of components are equal $\mu^{(2)}$ and $\mu^{(3)}$.

In the interfacial system the local densities depend on the distance from the surface. Our aim is to determine the density profiles of all components. For this purpose we have extended the density functional theory developed by Yu and Wu [23–26]. This approach is based on the fundamental measure theory of Rosenfeld [56] and the first-order perturbation theory of Wertheim [57]. The computational scheme used in this work is described in Appendix A.

We can use the model presented above to the chromatographic system consisting of the chemically bonded phase ("1"), the solute ("2") and the solvent ("3"). However, in analytical applications of chromatography the concentration of a sample is infinitely low while the mole fraction of the solvent is very high. In such a situation an accuracy of numerical determination of the solute density profiles can be unsatisfactory. An attempt to solve this problem has been postponed to our future work. Instead, we adapted our method to the so-called "continuum-solvent" model.

According to this concept all molecular species are immersed in a continuous medium that moderates molecular interactions in the system. We treat both components "2" and "3" as the solutes which densities are low and comparable. The parameter characterizing interactions between grafted polymer segments ($\varepsilon^{(11)}$) is used for modeling the solvent conditions. For "good solvents" the segment–solvent contacts are more favorable than contacts between segments of grafted chains. Notice that for $\varepsilon^{(11)} = 0$ the net segment–segment interactions are repulsive. In "poor solvent" the effective interactions are attractive and can even lead to partial collapse of chains. We model such conditions assuming high values of $\varepsilon^{(11)}$. In the same way interactions of the solutes with the grafted chains can be controlled (via the parameters $\varepsilon^{(k1)}$). This leads to considerable limitation of a number of system parameters.

In our theory the principal driving force for the retention is an attraction of the solute by the polymer chains. This approach is consistent with the results published by Ranutuga and Carr [58]. They have analyzed the thermodynamic functions estimated from the experimental data and came to conclusion that the retention is due mainly to enthalpy dominated liopophilic interactions of solutes with the stationary phase.

Each theory is based on a simplified model that mimics a real process. The model should be as close to reality as possible, but tractable theoretically. The model involves only the most important parameters characterizing the system. However, to a great extent, a choice of these parameters is intuitive. An agreement of theoretical results with relevant experiments should be the final test for the model.

Now, we would like to discuss assumptions introduced in our model. We begin with discussion the simplifications connected with the bonded phase. First of all, we use a very simple model of polymer molecules. The bonds between tangentially jointed spherical monomers have fixed length and are allowed to rotate freely. In other words, this is an idealization which neglects the torsional rigidity of polymer backbone bonds. Despite this simplification the model can give an accurate coarse-grained description of the large scale properties of real polymers. However, the "effective segment size" has to be adjusted carefully. Such a coarse-grained segment is always larger than monomer (it usually corresponds to at least 2.5 real monomers). The chromatographic bonded phases contains relatively short alkyl chains. On this length scale the use of this concept is not sufficiently justified. Therefore, we assume that the monomer – the segment of a chain – corresponds, more or less, to one methylene group.

In real chemically bonded phases the grafted ends of polymers are strictly fixed at active sites on the wall. In our model the chains are only forced to being at a certain distance from the surface. These chains are "annealed" on the surface but they can move within the *xy*-plane. Actually, the model corresponds to the strong physical adsorption of polymers. This model is considerably easier to handle theoretically. Using the implemented computational method one obtains only average segment densities of grafted chains in the *xy*-plane. Molecular simulations performed for the "anchored" and "annealed" chains have shown that for relatively dense bonded phases their density profiles differ only slightly [29,59]. Moreover in real systems polymers are grafted to the surface via siloxane bridges. Apart from the grafted chains, there are short branches, typically methylene groups, at the anchoring points. We do not take into account the structure of such bonding groups. In the model attractive interactions of all components with the solid surface are also neglected.

In the reversed phase chromatography binary solvents are usually used. The continuum-solvent model used in this work is a crude approximation of the real mobile phases. It is well-known that the retention depends strongly on a composition of the mobile phase. These effects cannot be analyzed explicitly in the framework of the continuum-solvent model. However, assuming different values of the energy parameters for different mixed solvents one can, to certain degree, take into account the composition of the mobile phase. Nevertheless, it is the most important limitation of this work.

Moreover, typical mobile phase are aqueous solutions with organic modifiers. In such solutions hydrogen-bonding interactions play a considerable role. These interactions are neglected in the model.

We focus our attention on a role of stationary phase in the retention process. The stationary phase contribution is almost ignored in a very popular solvophobic theory [60,61]. This model is based on the premise that the net interactions in the mobile phase are more significant than those in the stationary phase. On the contrary, on our approach the retention is dominated by interactions in the bonded phases. We will show that numerous important features of the retention can be interpreted in the framework of our theory.

2.2. Chromatographic systems

According to the model discussed above the whole system is treated as one phase. The densities of adsorbed species gradually change with the distance z from the surface and tend to their bulk values for z large enough. In order to apply the theory to the retention process, it is necessary to divide formally the systems into two phases: the stationary phase (surface phase) and the mobile (bulk) phase, because the distribution of solutes between these phases is an essence of chromatographic separation. However, the location of the dividing surface is rather arbitrary and several method for its estimation have been proposed [1,5,7,39,40,62].

In chromatographic experiments the observed retention is customary expressed as the retention factor $k_{S'}$, which is the number of solute molecules ("S") in the stationary phase divided by the number of solute molecules the mobile phase. The retention factor $k_{S'}$ is related to thermodynamically significant distribution ratio k_S, defined as the corresponding ratio of solute concentrations in the two phases:

$$K_S = \frac{\rho_{stat}^{(S)}}{\rho_b^{(S)}}, \tag{9}$$

where $\rho_{stat}^{(S)}$ is the average solute density in the stationary phase and $\rho_b^{(S)}$ is its density in the mobile (bulk) phase ($S=k=2$, 3):

$$\rho_{stat}^{(S)} = \frac{1}{h_s}\int_0^{h_s} \rho^{(S)}(z)\,dz \tag{10}$$

and $z=h_s$ denotes a position of the dividing surface.

The retention factor is given by

$$k'_S = K_S \Phi, \tag{11}$$

where Φ is the phase ratio, i.e., the ratio of the volumes of stationary and mobile phases:

$$\Phi = \frac{V_s}{V_m} = \frac{V_s}{(V-V_m)} = \frac{h_s}{(h-h_s)} = ch_s, \tag{12}$$

where V_s (h_s), V_m (h_m) and V (h) are the volumes (the thicknesses, $h=V/A$) of the stationary phase, the mobile phase and the total volume of the system (the column length), respectively. The phase ratio depends on various system parameters, such as the chain length, the nature of the eluent, the grafting density and temperature. A comparison of the experimental k'_S value with theoretically derived the distribution ratios K_S needs to take into account possible changes in the phase ratio Φ with the system variables. However, the optimal experimental determination of the phase ratio has been a matter of numerous discussions [1,5,7,39,63].

The volume of the mobile phase is much larger than the volume of the stationary phase, so $V_m \gg V_S$ ($h_m \gg h_s$). Therefore, the relative changes in the volume of the mobile phase are small and $(h-h_s)$ is approximately constant ($c=1/(h-h_s)$). Following Bohmer et al. [7] we define the "reduced" retention factor as:

$$k_S = h_s K_S = \frac{k'_S}{c}. \tag{13}$$

The "true" retention factor $k_{S'}$ is proportional to the reduced retention factor k_S. The value of the constant c depends on the characteristics of chromatographic column while the parameter h_s is an equilibrium property of the grafted layer. Because the boundary between mobile and stationary phases is not sharp, the thickness of stationary phase h_s must be defined explicitly. Bohmer et al. [7] assumed that h_s is equal to the hydrodynamic layer thickness that can be calculated in terms of theory given by Scheutjens et al. [63]. Combining Eqs. (9)–(13) we obtain the following expression for the reduced retention factor:

$$k_S = \frac{1}{\rho_b^{(S)}}\int_0^{h_s} \rho^{(S)}(z)\,dz. \tag{14}$$

In this work we assume that the dividing surface is located at the distance from the surface at which the local density of adsorbed fluid differs from its bulk value no more than 1%. This choice is explained below.

3. Results and discussion

3.1. Structure of the bonded phase

We start with the analysis of the structure of chemically bonded phases in different systems. We assume that the "effective height" of the brush (D_{eff}) is treated as the stationary phase thickness (h_s). Fig. 1 shows the density profiles of end-grafted chains for different chain lengths, grafting densities and energies of segment–segment interactions. All profiles have Dirac delta peaks at $z=\sigma^{(1)}/2$, which correspond to the pinned segments, these peaks are cut in Fig. 1.

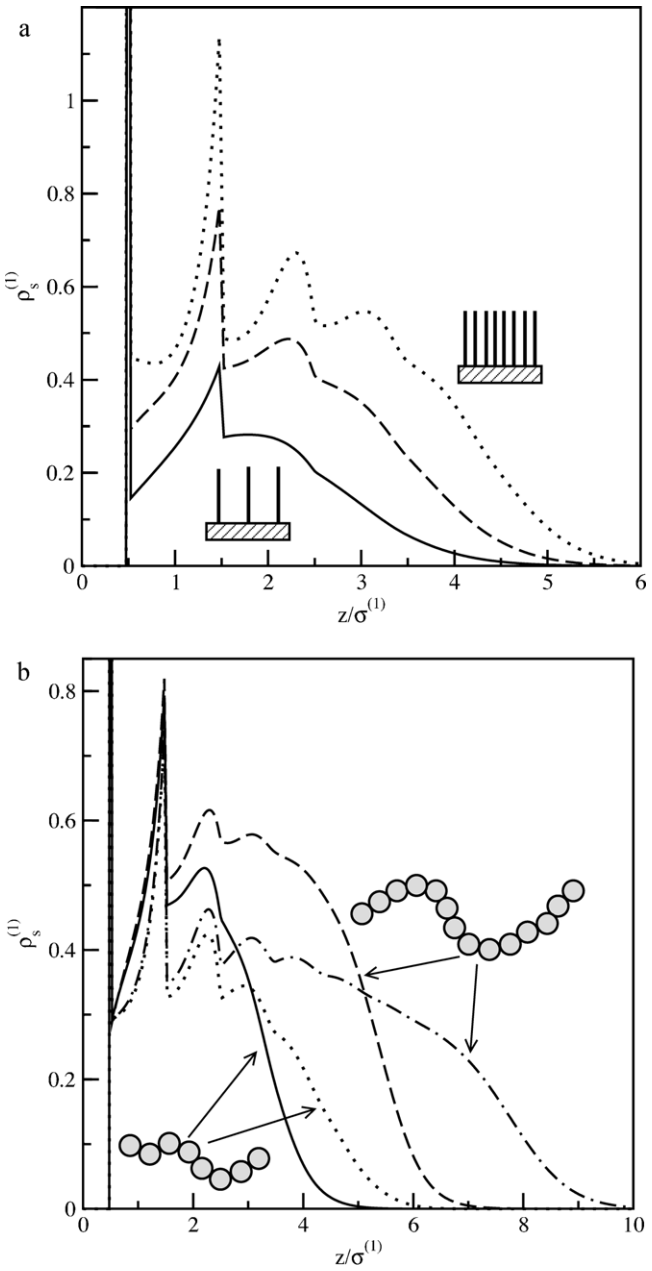

Fig. 1. Total segment density profiles of the chemically bonded phase. Parameters: (a) $\varepsilon^{(kl)}=0.33$, (k, $l=1$, 2, 3; $S=2$, 3), $M_1=8$, $M_2=3$, $M_3=1$, $\rho_{bs}^{(2)}=\rho_{bs}^{(3)}=0.05$ and $\rho_1=0.1$ (the solid line), 0.2 (the dashed line), 0.3 (the dotted line); (b) $\rho_1=0.2$, $M_1=8$ and $\varepsilon^{(11)}=0.4$ (the solid line), $\varepsilon^{(11)}=0.004$ (the dotted line), $M_1=14$ and $\varepsilon^{(11)}=0.4$ (the dashed line), and $\varepsilon^{(11)}=0.004$ (the dotted–dashed line).

The graphical symbols in Fig. 1a indicate the profiles for the highest and the lowest surface coverages. One see that an increase of grafting density causes a considerable rise of the brush height. Because of entropic effects the chains are repelled from the surface and they become more stretched. For low grafting densities polymer density profiles achieve maximum and then decrease almost monotonically when a distance from the surface increases. In the case of dense bonded phases the liquidlike structures with peaks corresponding to successive layers of polymer segments are observed. The influence of attractive segment–segment interactions on the structure of polymer film is shown in Fig. 1b. As it has been already mentioned, the attractive interactions between polymer segments ($\varepsilon^{(11)}$) mimic the "poor solvent regime". The attractive

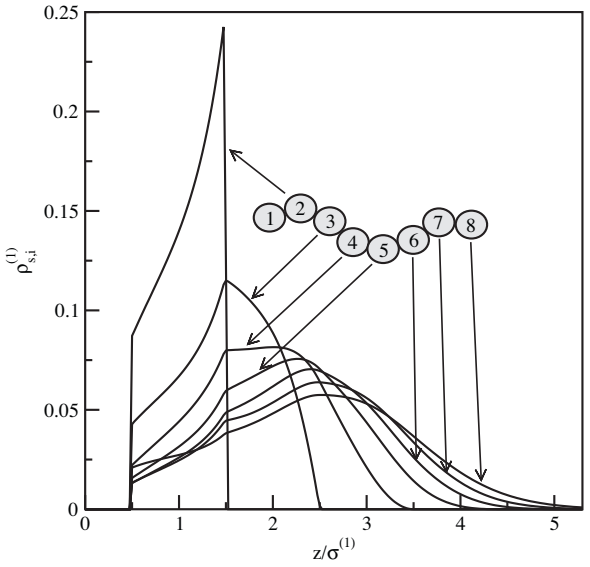

Fig. 2. Density profiles of individual segments of grafted chains. Parameters: $\varepsilon^{(kl)} = 0.33$, ($k$, $l = 1, 2$; $S = 2$), $M_1 = 8$, $M_2 = 2$, $\rho_{bs}^{(2)} = 0.01$, and $\rho_1 = 0.15$.

segment–segment interactions lead to folding the chains and the brush height decreases. This effect is more visible for longer chains. However, under assumed conditions the changes in the structure of bonded phase are not drastic. The phase collapse is not observed. This is in accordance with the spectroscopic studies which have not shown considerable solvent-induced conformational changes of bonded chains [42–44].

Further information about the structure of the bonded phase is provided by an analysis of profiles of particular segments (Fig. 2). In a completely stretched chain the segment numbered as n is located at the distance $(n + 1/2)\sigma^{(1)}$. For the considered system the maximum of the segment density is considerably shifted towards the solid surface. The distance between these two positions increases with increasing segment number. This suggests that parts of chains immediately connected with the bonding segment have a larger preference to align themselves perpendicularly to the surface. However, the "chain tails" take on the folded configurations. One can say that the chain order is smallest near the free ends where numbers of normal and lateral bonds are similar. The conclusions following from the above discussion are consistent with the general trends supported by numerous experimental measurements [42–54]. In our previous papers [29,30] we have shown that the theoretical profiles of bonded phases approximated the results of Monte Carlo simulations with a very good accuracy. Summarizing, one can state that the density functional theory quite well predicts the structure of bonded phases.

3.2. Distribution of the solute in the stationary phase

The density profiles of selected solutes and different bonded phases are presented Figs. 3–5. All calculations were performed for solutes built of the segments of the same size ($\sigma^{(3)} = \sigma^{(2)} = \sigma^{(1)}$).

The influence of the grafted chain length and the grafting density on the distribution of spherical solute molecules within the bonded phase is shown in Fig. 3. The "effective height" of the brush depends upon the grafting density. We have found that for shorter chains (Fig. 3a) the effective heights are $D_{eff} = 4.35$ and $D_{eff} = 4.45$, whereas for longer grafted chains (Fig. 3b) they are $D_{eff} = 7.63$ and $D_{eff} = 10.04$ for $\rho_1 = 0.15$ and $\rho_1 = 0.3$, respectively. In Fig. 3a and b the vertical lines indicate the brush boundaries. One can see that at low grafting densities (dashed lines) solute molecules penetrate into the bonded

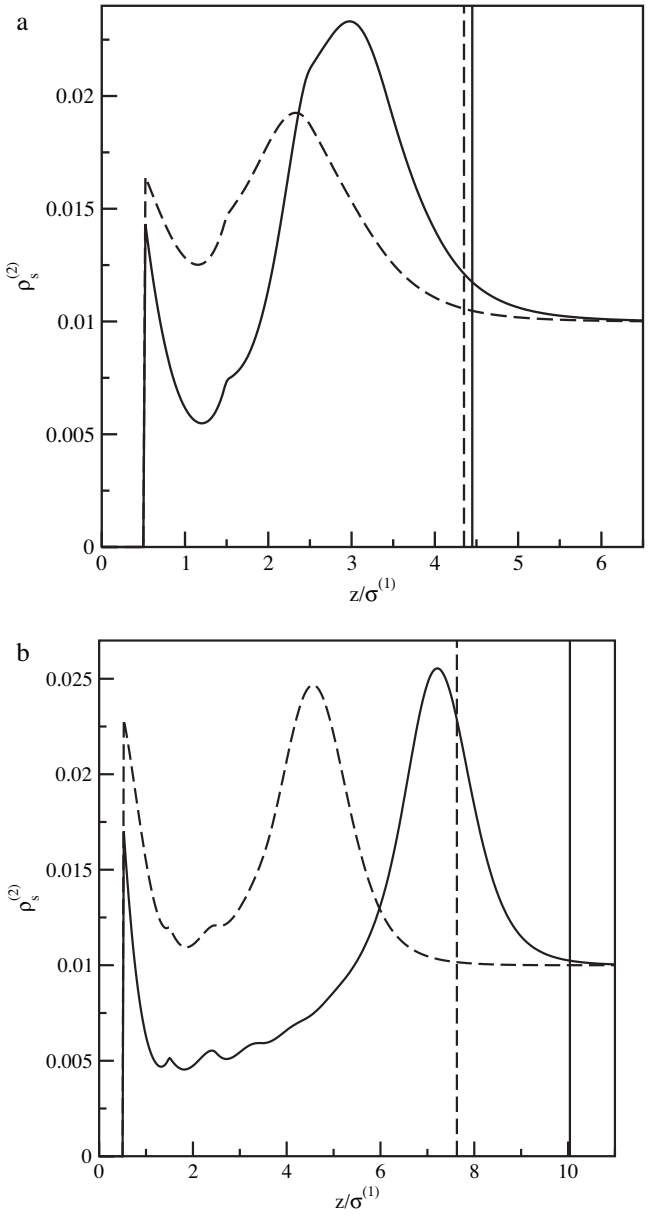

Fig. 3. Density profiles of spherical solutes. Parameters: $\varepsilon^{(kl)} = 0.5$, (k, $l = 1, 2$; $S = 2$), $\rho_1 = 0.15$ (dashed lines) and $\rho_1 = 0.3$ (solid lines); The vertical lines indicate the brush boundaries; (a) $M_1 = 5$; (b) $M_1 = 15$.

phase and a density maximum is observed in its core part. In the case of dense bonded phase (solid lines) this peak is located in the outer part of the polymer film and the solute density in the middle region of the bonded phase is even lower than in the mobile phase. It is interesting to note that for longer polymers the height of the peak is almost independent of the grafting density (Fig. 3b). The distribution of solute in the bonded phase becomes less "homogeneous" with increasing chain length and grafting density.

The effects of solute-bonded phase interactions on the solute sorption are shown in Fig. 4. For weak interactions with grafting chains spherical molecules adsorbed do not penetrate into the brush. However, in the case of stronger interactions with the polymer film the solute concentration in the stationary phase becomes higher than in the mobile phase.

In Fig. 5 the total segment density profiles of several linear solutes are plotted. Fig. 5a illustrates the influence of grafted chain length on the distribution of dimeric solute molecules in the sta-

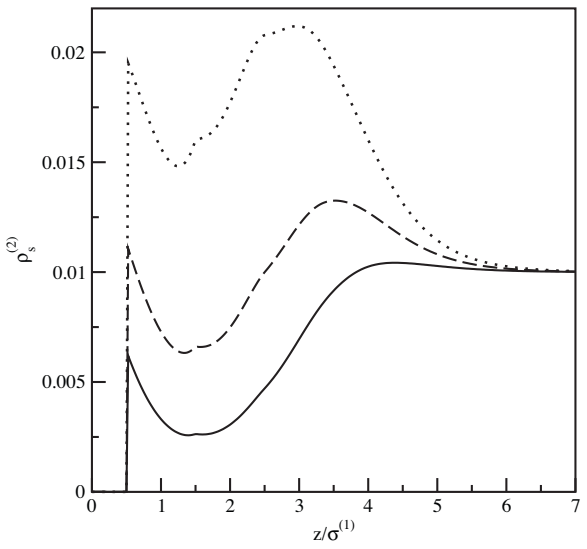

Fig. 4. Density profiles of spherical solutes ($S=2$). Parameters: $M_1=8$, $\rho_1=0.15$, $\varepsilon^{(11)}=\varepsilon^{(22)}=0.33$, $\varepsilon^{(12)}=0.17$ (the solid line), 0.33 (the dashed line), and 0.5 (the dotted line).

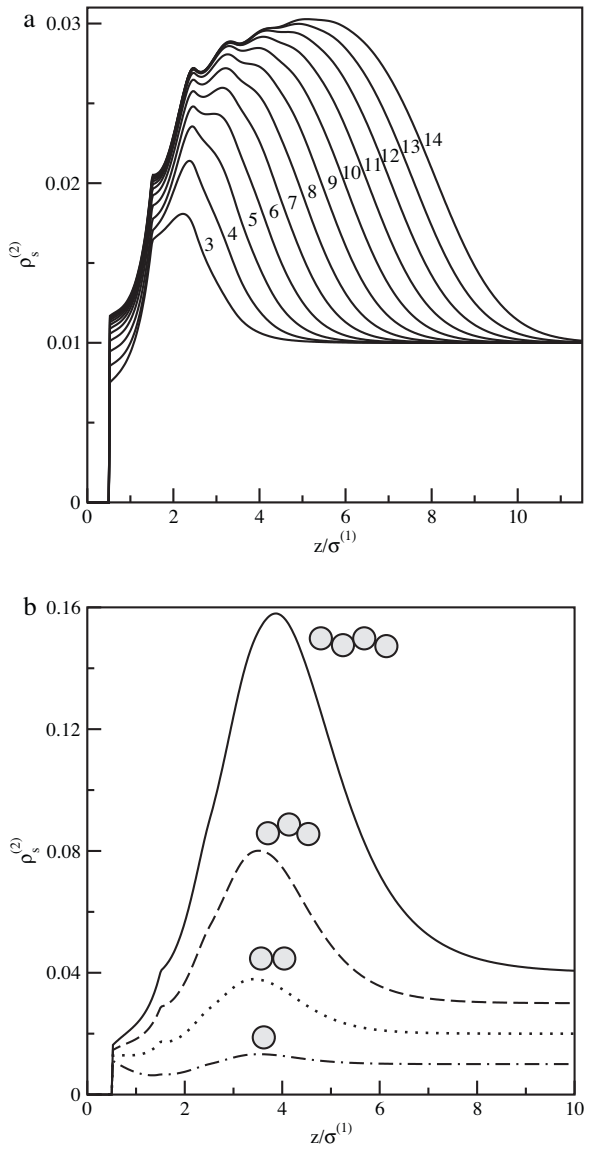

Fig. 5. Segment density profiles of different short chains. Parameters: (a) $\varepsilon^{(kk)}=\varepsilon^{(23)}=0.004$, $\varepsilon^{(12)}=\varepsilon^{(13)}=0.4$, ($k=1, 2, 3$; $S=2, 3$), $\rho_1=0.2$, $\rho_{bs}^{(2)}=0.01$, $\rho_{bs}^{(3)}=0.005$, $M_2=2$, $M_3=1$ and $M_1=3, 4, \ldots, 14$; (b) $\varepsilon^{(kl)}=0.33$, ($k, l=1, 2$; $S=2$), $\rho_1=0.15$, $M_1=8$, and $M_2=1, 2, 3, 4$.

tionary phase. The dimers are located in the middle part of the polymer brush, where their density is almost constant. For longer grafted chains such a "homogeneous" region becomes wider. In contrast to spherical molecules, dimers can align with the grafted chains so they are more effectively retained. In Fig. 5b the segment density profiles of monomers, dimers, trimers and tetramers are compared. The number densities of all solutes in the bulk phase are the same. All solutes accumulate in the core part of bonded phase. The smaller molecules penetrate deeper into the polymer film. On the other hand, the densities of longer solutes in the bonded phase are higher because their interactions between surrounding polymer segments are stronger.

We have not found the bimodal behavior of the density profile of the nonpolar solute reported by Rafferty et al. [39]. They observed the "partitioning peak" in the middle of the bonded phase and the "adsorption peak" inside the interface between the stationary and mobile phases. However, our observations are consistent with the results of previous theoretical studies [7] in which, similarly as in our treatment, the mean field approximation was applied.

In all studied cases the bonded phases are highly inhomogeneous. One can divide the film into three parts: (i) the interfacial region that is located near the solid surface; (ii) the interface between the polymer brush and the mobile phase; and (iii) the "bulk" part of the bonded phase. Unfortunately, there is no strict method to quantify the thickness of the interface. The volume of the "bulk" stationary phase is comparable with volumes of the interfacial regions. This is particularly visible for low grafting densities. Moreover, there is no well-pronounced flat part in the segment density profile for the "bulk" region. Therefore, the use of the standard method [62] for a location of the Gibbs dividing surface is not precise. It should be also pointed out that solutes can adsorb "on the brush", where the polymer density is close to zero [1,2,29,30]. One can suppose that for strong solute-segment interactions these molecules retain in the stationary phase during a flow of the mobile phase. For these reasons we decided to make the stationary phase more extended. The position of the boundary between the stationary and the mobile phase is estimated from the analysis of the density profiles of solute molecules and we use the value at which the total solute density differs from its value in the bulk part of mobile phase no more than 1%.

3.3. Correlations with experiments

Now, we would like to test the theory comparing its predictions with the selected empirical dependencies. Fig. 6 illustrates an influence of the length of grafted chains and the grafting density on the distribution ratio (K_S) and on the reduced retention factor (k_S) for spherical solute molecules. As the chain length increases the distribution ratio increases to the maximum value and then gradually decreases. At low grafting densities the maximum values are achieved for much longer chains than for the dense bonded phase (Fig. 6a). In the case of high grafting densities a decrease in the distribution ratio is quite rapid for the long chains. However, the retention factor always increases with increasing chain length (Fig. 6b). Such a difference in the behavior of distribution coefficient and the retention ratio is a simple consequence of the considerable increase in the volume of stationary phase for longer chains. The comparison of the results presented in Fig. 6a and Fig. 6b clearly shows that changes in the phase ratio can strongly affect the retention. Moreover, for longer grafted chains the logarithm of the

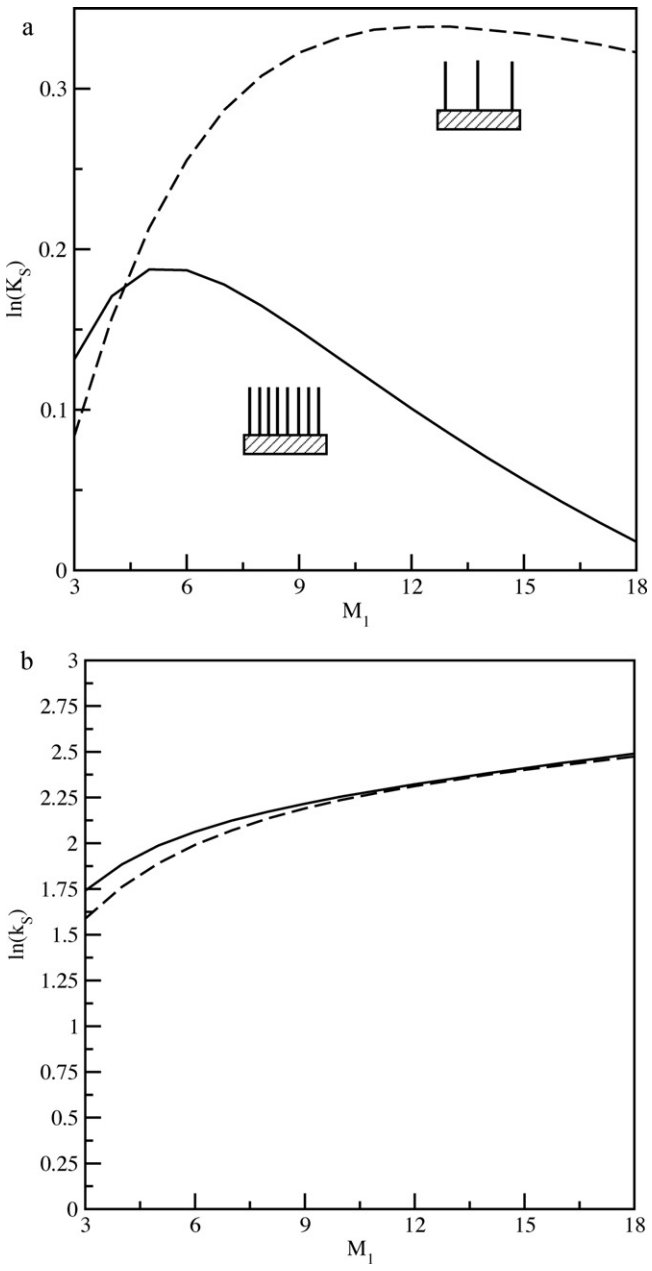

Fig. 6. The influence of grafted chain length on the distribution ratio K_S (a) and the reduced retention factor k_S (b) of spherical solute molecules. Parameters: $\varepsilon^{(kl)} = 0.5$, (k, $l = 1, 2$; $S = 2$), $\rho_{bs}^{(2)} = 0.01$, $\rho_1 = 0.15$ (dashed lines) and $\rho_1 = 0.3$ (solid lines).

retention factor increases almost linearly with increase in the number of segments in the bonded chains. Similar relations are found for linear molecules (Fig. 7). This observation is consistent with the experimental results obtained for nonpolar solutes [64–67].

Fig. 8 shows the dependencies of the reduced retention factors k_S on the grafting density. For low grafting densities the retention factor increases with the surface coverage of grafted chains. As the polymer film becomes sufficiently dense the chains start to hinder penetration of the brush and the retention factor remains constant or even decreases with a further increase in the polymer surface coverage. At higher grafting densities the distribution ratio decreases whereas the stationary-phase volume increases. When these effects approximately cancel, the plateauing retention with increasing grafting density is observed. However, as the effects connected with a decrease in the solute sorption dominate the retention factor decreases. The both types of relationships between

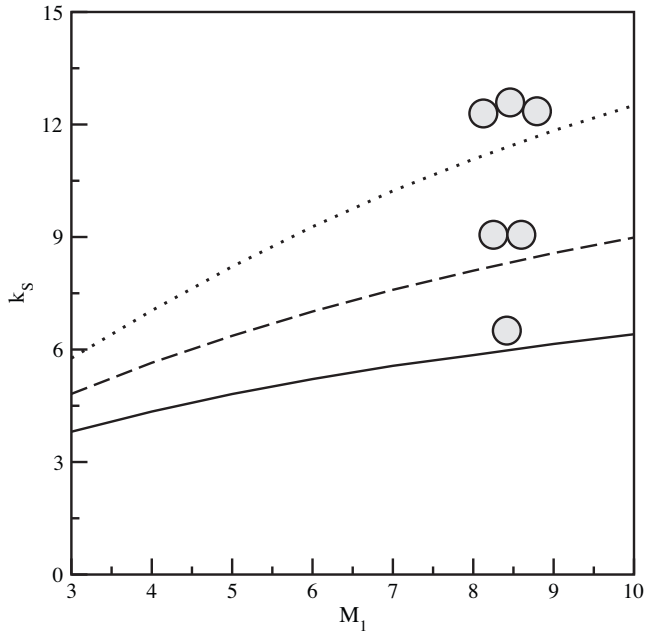

Fig. 7. The influence of grafted chain length on the reduced retention factor of short chains. Parameters: $\varepsilon^{(kl)} = 0.33$, ($k$, $l = 1, 2$; $S = 2$), $\rho_{bs}^{(2)} = 0.01$, $\rho_1 = 0.15$, and $M_2 = 1, 2, 3$.

the retention factor and the surface coverage have been observed in experiments [1,2,67–75].

Now, we would like to discuss the influence of the solute molecules size on the retention factor. At higher temperatures the $\ln(k_S)$ is a linear function of the solute size (Fig. 9). This result is in accordance with numerous experimental measurements [1,76–80]. However, at a low temperature we observe deviations from linear dependence between $\ln(k_S)$ and the solute size. When temperature decreases solute-bonded phase interactions become stronger. The slopes of the lines $\ln(k_S)$ vs. M_S increase with increas-

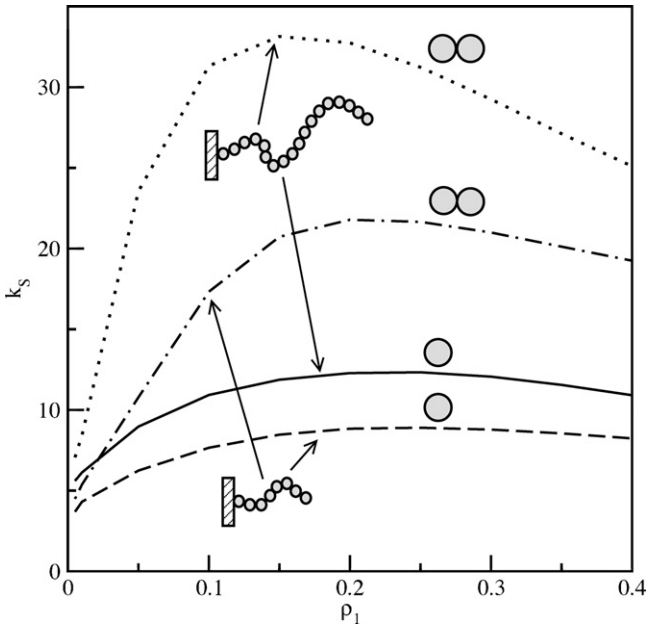

Fig. 8. The influence of grafting density on the reduced retention factor. Parameters: $\varepsilon^{(kl)} = 0.5$, (k, $l = 1, 2$; $S = 2$), $\rho_{bs}^{(2)} = 0.01$ (monomer) and $\rho_{bs}^{(2)} = 0.02$ (dimer), and $M_1 = 8$, 18.

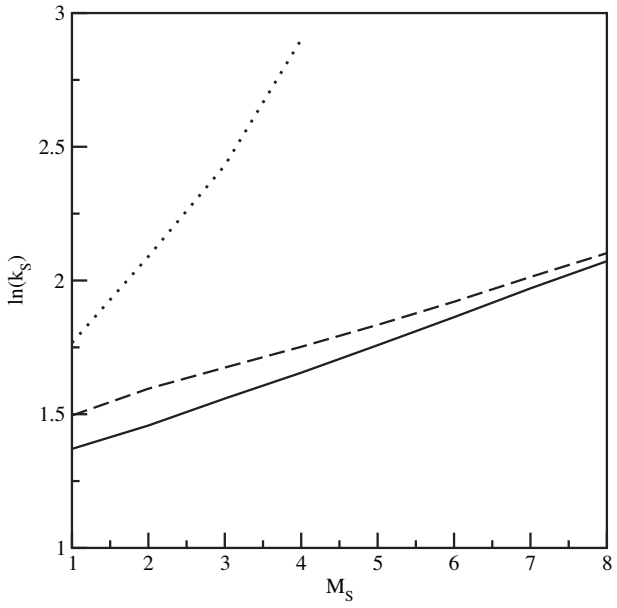

Fig. 9. The influence of solute size (M_2) on the reduced retention factor. Parameters: $M_1 = 8$, $\rho_{bs}^{(2)} = 0.01$; $\varepsilon^{(kl)} = 0.33$, and $\rho_1 = 0.15$ (the dotted line), $\varepsilon^{(kl)} = 0.2$, and $\rho_1 = 0.15$ (the dashed line), $\varepsilon^{(kl)} = 0.2$, and $\rho_1 = 0.3$ (the solid line); (k, $l = 1, 2$; $S = 2$).

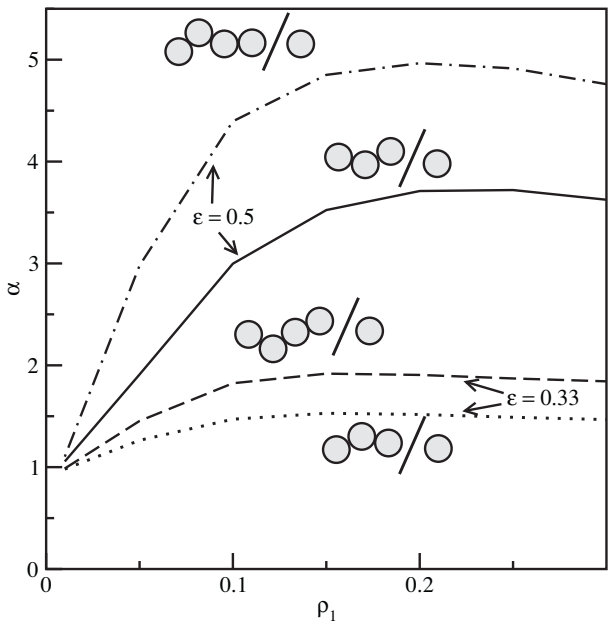

Fig. 11. The influence of grafting density on the separation factor for trimer/monomer and tetramer/monomer mixtures. Parameters: $M_1 = 8$, $\rho_{bs}^{(2)} = 0.005$, $\rho_{bs}^{(3)} = 0.015$ for trimer and $\rho_{bs}^{(3)} = 0.02$ for tetramer, $\varepsilon^{(kk)} = \varepsilon^{(23)} = 0.33$, $\varepsilon^{(12)} = \varepsilon^{(13)} = \varepsilon$, ($k = 1, 2, 3$; $S = 2, 3$); trimer/monomer: $\varepsilon = 0.33$ (the dotted line), $\varepsilon = 0.5$ (the solid line); tetramer/monomer: $\varepsilon = 0.33$ (the dashed line), $\varepsilon = 0.5$ (the dot–dashed).

ing effective attraction of the solute. These observations also match the experimental data [79,80].

Let us analyze the temperature effects in the retention process (Fig. 10). In all cases an increase of temperature causes a decrease of the retention factor. Almost linear dependence $\ln(k_S)$ vs. $1/T^*$ is found for small spherical molecules of the solute. This agrees with the experimental works [81–86]. However, for dimers and trimers a departure from linearity is observed. In this case the changes in entropy following from transfer the solute from the mobile to the inhomogeneous stationary phase can be significant and affect their retention.

Finally, we want to discuss an impact of the nature of chemically bonded phase on the selectivity. The separation factors calculated for different pairs of solutes are depicted in Figs. 11 and 12. We consider the separation of the solutes belonging to the same homologous series ($\varepsilon^{(12)} = \varepsilon^{(13)} = \varepsilon$). We assume that number segment densities of the solutes in the mobile phase are the same. One see in Fig. 11 that the separation factor α increases with the increasing surface coverage of bonded phase up to a certain threshold value for each solute pair. Subsequently, the separation factor stays approximately constant or slightly decreases. These predictions were confirmed by the experimental data [67].

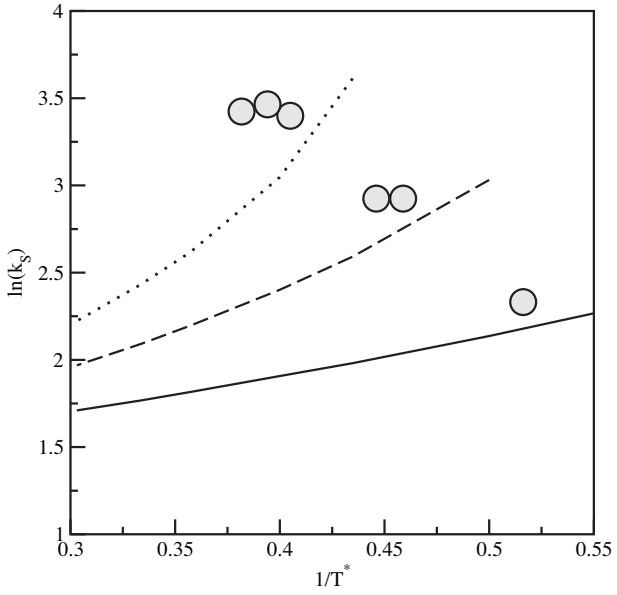

Fig. 10. The influence of temperature ($T^* = k_B T/\tilde{\varepsilon}^{(kl)}$) on the reduced retention factor. Parameters: $\tilde{\varepsilon}^{(kl)} = 1$, ($k$, $l = 1, 2$; $S = 2$), $M_1 = 8$, $\rho_1 = 0.15$, $\rho_{bs}^{(2)} = 0.01$ (monomer), $\rho_{bs}^{(2)} = 0.02$ (dimer) and $\rho_{bs}^{(2)} = 0.03$ (trimer).

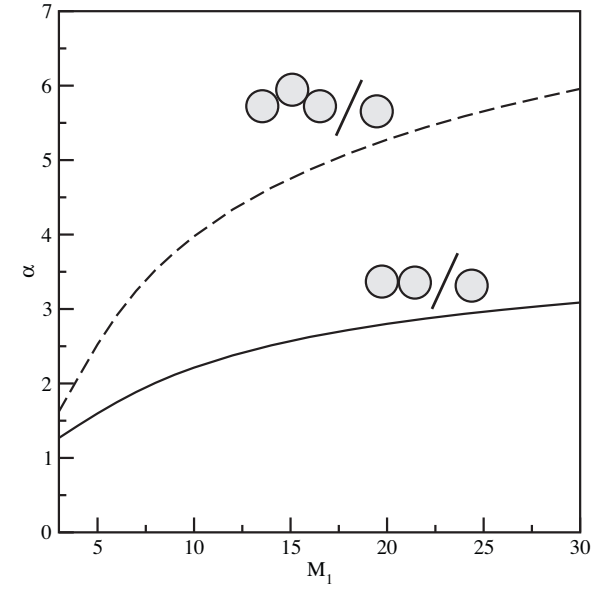

Fig. 12. The influence of grafted chain length on the separation factor for dimer/monomer and trimer/monomer mixtures. Parameters: $\varepsilon^{(kk)} = \varepsilon^{(23)} = 0.33$, $\varepsilon^{(12)} = \varepsilon^{(13)} = 0.5$, ($k$, $l = 1, 2, 3$; $S = 2, 3$), $\rho_1 = 0.15$, $\rho_{bs}^{(2)} = 0.005$, and $\rho_{bs}^{(3)} = 0.01$ for dimer and $\rho_{bs}^{(3)} = 0.015$ for trimer.

It should be, however, pointed out that the selectivity depends strongly on the energy parameter (ε) that characterizes the strength of attractive interactions of one segment (monomer) with the bonded phase. The separation factors shown in Fig. 11 are of the same order of magnitude as the experimental values measured by Colin et al. [79] for n-alkanes retained from methanol/water mobile phases on Hypersil ODS. The separation factor for the r-mer/monomer pair increases when the percent water increases [79]. Fig. 12 shows the influence of the grafted chains length on the separation factor for selected systems. For pairs of solutes considered here the separation factors increase with the increasing chain length. Similar experimental results were reported [64–67,87].

4. Conclusions

The density functional theory can be applied to retention of spherical and linear solutes in chromatography with chemically bonded phases. This method can be used either to gas chromatography or to reversed-phase liquid chromatography. We have demonstrated that the density functional theory well predicts the salient features of the process.

This study confirms that the structure of the stationary phase plays a major role in retention. The most important factors in determining the brush structure are the grafting density and interactions between anchored chains. The effective brush height increases with increasing grafting density because the chains align themselves more perpendicular to the surface. However, when attraction between polymer segments becomes stronger the grafted chains form coils and the brush height decreases. In the framework of a continuum solvent model the energy of segment–segment interactions can be used to mimic the "good" or "poor solvent conditions". Further information about the structure of bonded phase is provided by an analysis of the theoretical profiles of individual polymer segments.

We have determined the density profiles of spherical and linear solutes near the surface covered by polymer chains. The distribution of the solute molecules in the stationary phase has appeared to be highly heterogeneous. We have shown that variation in assumed parameters causes change in the mechanism of retention. The solute molecules can penetrate into the interior of the bonded phase or reside in the outer region of the brush. Under some circumstances the solute molecules are retained onto the bonded phase. This means that both partitioning and adsorption can play a key role in the retention process.

The theoretical prediction for dependencies of retention on the grafting density, the length of bonded chains and the solute size are consistent with numerous experimental results. At low grafting densities the retention factor increases, reaches a maximum and remains constant or gradually decreases. However, for longer bonded chains and larger solute molecules the retention becomes higher. The temperature effects following from the theory are also supported by experimental evidences.

We have confirm that the nature of the chemically bonded phase plays a role of fundamental importance in chromatographic separation. The separation factors calculated for different pairs of solutes depend considerably on the grafting density and the length of bonded chains.

The main limitation of the study is a fact that we involve the solvent-free model of the system. However, the theory can be extended to more sophisticated models. On the other hand, the simplicity of the approach, relatively small number of needed parameters is its good point. Nevertheless, in the future work we plan to consider solvent effects and analyze the role of hydrogen bonds in retention using theory of associating fluids [88].

Acknowledgment

This work was supported by the Ministry of Science and Higher Education of Poland under the Grant No. N N204 151237.

Appendix A.

The scheme contains the following steps: (i) construction of the free energy functional; (ii) construction of the thermodynamic potential functional; (iii) minimization of the thermodynamic potential; (iv) solution of the obtained set of Euler–Lagrange equations. This procedure leads to the equilibrium density profiles of grafted polymer segments and segments of fluid molecules.

The Helmholtz energy functional is decomposed as the sum of ideal and excess terms $F = F_{id} + F_{ex}$. The ideal part of the free energy functional is known exactly as:

$$\beta F_{id} = \beta \sum_{k=1}^{3} \left[\int d\mathbf{R}_k \rho^{(k)}(\mathbf{R}_k) V_B(\mathbf{R}_k) + \int d\mathbf{R}_k \rho^{(k)}(\mathbf{R}_k) [\ln(\rho^{(k)}(\mathbf{R}_k)) - 1] \right], \tag{A.1}$$

where $\rho^{(k)}(\mathbf{R}_k)$ is the local density of kth molecules. The total segment density is related to the multidimensional density profile of the chains, $\rho^{(k)}(\mathbf{R}_k)$, by

$$\rho_s^{(k)}(r) = \sum_{j=1}^{M_k} \rho_{s,j}^{(k)}(r) = \sum_{j=1}^{M_k} \int d\mathbf{R}_k \delta(r - r_j) \rho^{(k)}(\mathbf{R}_k). \tag{A.2}$$

The excess free energy takes into account the contribution from hard sphere repulsion (F_{hs}), the intramolecular chain connectivity (F_c) and van der Waals attraction (F_{att}), so

$$F_{ex} = F_{hs} + F_c + F_{att}. \tag{A.3}$$

The excess free energy term due to hard-sphere contribution is evaluated from the fundamental measure theory [56]:

$$F_{hs} = \int \Phi_{hs}(r)\, dr, \tag{A.4}$$

with

$$\Phi_{hs} = -n_0 \ln(1 - n_3) + \frac{n_1 n_2 - \mathbf{n}_1 \cdot \mathbf{n}_2}{1 - n_3} + n_2^3 (1 - \xi^2)^3 \frac{n_3 + (1 - n_3)^2 \ln(1 - n_3)}{36\pi n_3^2 (1 - n_3)^2}, \tag{A.5}$$

where $\xi(\mathbf{r}) = |\mathbf{n}_2(\mathbf{r})|/n_2(\mathbf{r})$. The scalar, n_i, i=0, 1, 2, 3 and vector, $\mathbf{n}_i$, i = 1, 2 weighted densities are convolutions of the total segment densities and corresponding weight functions proposed in Ref. [56].

Following the first-order perturbation theory of Wertheim [57] the excess free energy functional, F_c, is represented by

$$F_c = \sum_{k=1}^{3} \frac{1 - M_k}{M_k} \int d\mathbf{r} n_0^{(k)} \zeta \ln[y_{(hs)}^{(k)}(\sigma^{(k)})], \tag{A.6}$$

where

$$y_{hs}^{(k)}(\sigma^{(k)}) = \frac{1}{1 - n_3} + \frac{n_2 \sigma^{(k)} \zeta}{4(1 - n_3)^2} + \frac{(n_2 \sigma^{(k)})^2 \zeta}{72(1 - n_3)^3}, \tag{A.7}$$

for $\zeta = 1 - \mathbf{n}_2^{(k)} \cdot \mathbf{n}_2^{(k)} / (n_2^{(k)})^2$ [29].

Finally, the excess free energy resulting from attractive interactions is obtained within the mean field approximation:

$$F_{att} = \frac{1}{2}\sum_{k=1}^{3}\int d\mathbf{r}_1 d\mathbf{r}_2 \rho_s^{(k)}(\mathbf{r}_1)\rho_s^{(k)}(\mathbf{r}_2)u^{(kk)}(\mathbf{r}_{12}) + \sum_{k=1,k<l}^{3}\int d\mathbf{r}_1 d\mathbf{r}_2 \rho_s^{(k)}(\mathbf{r}_1)\rho_s^{(l)}(\mathbf{r}_2)u^{(kl)}(\mathbf{r}_{12}). \quad (A.8)$$

The thermodynamic potential for the system in which the total number of grafted chains is fixed can be expressed as:

$$Y = F[\rho^{(1)}(\mathbf{R}_1), \rho^{(2)}(\mathbf{R}_2), \rho^{(3)}(\mathbf{R}_3)] + \int d\mathbf{R}_1 \rho^{(1)}(\mathbf{R}_1)(\nu^{(1)}(\mathbf{R}_1)) + \sum_{k=2,3}\int d\mathbf{R}_k \rho^{(k)}(\mathbf{R}_k)(\nu^{(k)}(\mathbf{R}_k) - \mu^{(k)}). \quad (A.9)$$

The constancy of the grafting density leads to the following condition:

$$\int_0^{(M_1+1/2)\sigma^{(1)}} dz \rho_{s,i}^{(1)}(z) = \rho_1, \quad (A.10)$$

where ρ_1 is the assumed grafting density of the chains.

The segment density profiles are obtained by minimizing the thermodynamic potential Y. For systems with density distributions varying only in z direction the segment densities of chain molecules are given by

$$\rho_{s,i}^{(k)}(z) = \tilde{C}_k \exp[-\beta\lambda_i^{(k)}(z)]G_i^{(k,L)}(z)G_{M_k+1-i}^{(k,R)}(z), \quad (A.11)$$

for

$$\lambda_i^{(k)}(z_i) = \frac{\delta F_{ex}}{\delta\rho_s^{(k)}(z_i)} + \nu_{si}^{(k)}(z_i) \quad (A.12)$$

where the functions $G^{(k,P)}(z)$, $P = L, R$ are calculated using the following recurrence relations:

$$G_i^{(k,L)}(z) = \int dz' \exp[-\beta\lambda_{i-1}^{(k)}(z)]\frac{\theta(\sigma^{(k)} - |z - z'|)}{2\sigma^{(k)}}G_{i-1}^{(k,L)}(z'), \quad (A.13)$$

and

$$G_i^{(k,R)}(z) = \int dz' \exp[-\beta\lambda_{M_k-i+2}^{(k)}(z)]\frac{\theta(\sigma^{(k)} - |z - z'|)}{2\sigma^{(k)}}G_{i-1}^{(k,L)}(z'), \quad (A.14)$$

for $i = 2, 3, \ldots, M_k$ and with $G^{(k,L)}(z) = G^{(k,R)}(z) \equiv 1$. For $k = 2$ and 3 the quantities $\tilde{C}_k$, entering Eq. (A.11) are $\tilde{C}_k = \exp[\beta\mu^{(k)}]$, whereas $\tilde{C}_1$ is evaluated from Eq. (A.10).

References

[1] J.G. Dorsey, K.A. Dill, Chem. Rev. 89 (1989) 331.
[2] L.C. Tan, P.W. Carr, J. Chromatogr. A 775 (1997) 1.
[3] M. Jaroniec, D.E. Martire, M. Borówko, Adv. Colloid Interface Sci. 22 (1985) 177.
[4] P.J. Schoenmakers, Optimization of Chromatographic Selectivity, A Guide to Method Development, J. Cromatographic Library, vol. 35, Elsevier, Amsterdam, 1986.
[5] D.E. Martire, R.E. Boehm, J. Phys. Chem. 87 (1983) 1045.
[6] K.A. Dill, J. Phys. Chem. 91 (1987) 1980.
[7] M.R. Bohmer, L.K. Koopal, R. Tijssen, J. Phys. Chem. 95 (1991) 6285.
[8] F.A.M. Leermakers, H.J.A. Philipsen, B. Klumperman, J. Chromatogr. A 959 (2002) 37.
[9] G.J. Fleer, A.A. Cohen Stuart, J.M.H.M. Scheutjens, T. Cosgrove, B. Vincent, Polymers at Interfaces, Chapman and Hall, London, 1993.
[10] R.R. Netz, D. Andelman, Phys. Rep. 380 (2003) 1.
[11] S. Alexander, J. Phys. (France) 38 (1977) 983.
[12] P.G. de Gennes, Macromolecules 13 (1980) 1069.
[13] S.T. Milner, T.A. Witten, M.E. Cates, Europhys. Lett. 5 (1988) 413.
[14] S.T. Milner, T.A. Witten, M.E. Cates, Macromolecules 21 (1988) 2610.
[15] S.T. Milner, Science 251 (1991) 905.
[16] E.B. Zhalina, O.V. Borisov, V.A. Pryamitsyn, T.M. Birshtein, Macromolecules 24 (1991) 140.
[17] M.A. Carignano, I. Szleifer, J. Chem. Phys. 100 (1994) 3210.
[18] M.A. Carignano, I. Szleifer, Macromolecules 28 (1995) 3197.
[19] M.A. Carignano, I. Szleifer, J. Chem. Phys. 102 (1995) 8662.
[20] J.D. McCoy, M.A. Teixeira, J.G.J. Curro, J. Chem. Phys. 113 (2001) 4289.
[21] J.D. McCoy, Y. Ye, J.G.J. Curro, J. Chem. Phys. 117 (2002) 2075.
[22] Y. Ye, J.D. McCoy, J.G.J. Curro, J. Chem. Phys. 119 (2003) 555.
[23] Y.-X. Yu, J. Wu, J. Chem. Phys. 117 (2002) 2368.
[24] Y.-X. Yu, J. Wu, J. Chem. Phys. 117 (2002) 10156.
[25] Y.-X. Yu, J. Wu, J. Chem. Phys. 118 (2003) 3835.
[26] D.P. Cao, J. Wu, Langmuir 22 (2006) 2712.
[27] P. Bryk, O. Pizio, S. Sokoł owski, J. Chem. Phys. 122 (2005) 194906.
[28] O. Pizio, K. Bucior, A. Patrykiejew, S. Sokołowski, J. Chem. Phys. 123 (2005) 214902.
[29] M. Borówko, W. Rżysko, S. Sokołowski, T. Staszewski, J. Chem. Phys. 126 (2007) 214703.
[30] M. Borówko, W. Rżysko, S. Sokołowski, T. Staszewski, J. Phys. Chem. 113 (2009) 4763.
[31] S.J. Klatte, T.L. Beck, J. Chem. Phys. 97 (1993) 5727.
[32] S.J. Klatte, T.L. Beck, J. Chem. Phys. 99 (1995) 160524.
[33] I. Yarovsky, M.I. Aguilar, M.T. Hearn, Anal. Chem. 68 (1996) 1974.
[34] K.A. Lippa, L.C. Sander, R.D. Mountain, Anal. Chem. 77 (2005) 7862.
[35] S.J. Klatte, T.L. Beck, J. Chem. Phys. 100 (1996) 5931.
[36] J.T. Sluster, R.D. Mountain, J. Phys. Chem. 103 (1999) 1354.
[37] K. Ban, Y. Saito, K. Jinno, Anal. Sci. 21 (2005) 397.
[38] J.L. Rafferty, J.I. Siepmann, M.R. Schure, J. Chromatogr. A 1204 (2008) 11.
[39] J.L. Rafferty, J.I. Siepmann, M.R. Schure, J. Chromatogr. A 1204 (2008) 20.
[40] J.L. Rafferty, J.I. Siepmann, M.R. Schure, Anal. Chem. 80 (2008) 6214.
[41] J.L. Rafferty, J.I. Siepmann, M.R. Schure, J. Chromatogr. A 1216 (2009) 2320.
[42] C.A. Doyle, T.J. Vickers, C.K. Mann, J.G. Dorsey, J. Chromatogr. A 877 (2000) 25.
[43] C.A. Doyle, T.J. Vickers, C.K. Mann, J.G. Dorsey, J. Chromatogr. A 877 (2000) 41.
[44] C.J. Orendorf, M.W. Ducey, J.E. Pemberton, L.C. Sander, Anal. Chem. 75 (2003) 3360.
[45] J.E. Pemberton, M. Ho, C.J. Orendorf, J. Chromatogr. 913 (2001) 249.
[46] Z. Liao, J.E. Pemberton, J. Chromatogr. A 1193 (2008) 60.
[47] Z.H. Liao, J.E. Pemberton, Anal. Chem. 80 (2008) 2911.
[48] R.C. Ziegler, G.E. Maciel, J. Am. Chem. Soc. 113 (1991) 6349.
[49] M. Pursch, S. Strohschein, H. Handel, K. Albert, Anal. Chem. 68 (1996) 386.
[50] M. Pursch, L.C. Sander, H.J. Egelhaaf, M. Raitza, S.A. Wise, D. Oelkrug, K. Albert, J. Am. Chem. Soc. 121 (1999) 3201.
[51] M.E. Montgomery, M.A. Green, M.J. Wirth, Anal. Chem. 64 (1992) 1170.
[52] M.J. Wirth, D.J. Swinton, M.D. Ludes, J. Phys. Chem. B 107 (2003) 6258.
[53] M.C. Henry, L.K. Wolf, M.C. Messmer, J. Phys. Chem. B 107 (2003) 2765.
[54] L.C. Sander, C.J. Glinka, S.A. Wise, Anal. Chem. 62 (1990) 1099.
[55] J.D. Weeks, D. Chandler, H.C. Andersen, J. Chem. Phys. 54 (1971) 5237.
[56] J. Rosenfeld, Phys. Rev. Lett. 63 (1989) 980.
[57] M.S. Wertheim, J. Chem. Phys. 87 (1987) 7323.
[58] R.J. Ranutuga, P.W. Carr, Anal. Chem. 72 (2000) 5679.
[59] D.T. Lai, K. Binder, J. Chem. Phys. 97 (1992) 586.
[60] W.R. Melander, Cs. Horvath, in: Cs. Horvath (Ed.), High Performance Liquid Chromatography, Advances and Perspectives, vol. 2, Academic Press, New York, 1980, p. 201.
[61] L.R. Snyder, J.W. Dolan, P.W. Carr, J. Chromatogr. A 1060 (2004) 77.
[62] J. Ościk, Adsorption, Ellis Horwood Publisher, Chichester, 1979.
[63] J.M.H.M. Scheutjens, G.J. Fleer, M.A. Cohen Stuart, Colloids Surf. 21 (1986) 285.
[64] R.E. Majors, M.J. Hopper, Journal of Chromatographic Science 12 (1974) 767.
[65] K.K. Unger, N. Becker, P. Roumeliotis, J. Chromatogr. 125 (1976) 115.
[66] H. Hemetsberger, W. Maasfeld, H. Ricken, Chromatographia 9 (1976) 303.
[67] M.C. Hennion, C. Picard, M. Caude, J. Chromatogr. 166 (1978) 21.
[68] M.L. Miller, R.W. Linton, S.G. Bush, J.W. Jorgenson, Anal. Chem. 56 (1984) 2204.
[69] S.A. Tomellini, S.H. Shu, F.D. Fazio, R.A. Hartwick, J. High Resolut. Chromatogr., Chromatogr. Commun. 8 (1985) 337.
[70] E.J. Kikta, E. Grushka, Anal. Chem. 48 (1976) 1098.
[71] N. Tanaka, H. Goodell, B.L. Karger, J. Chromatogr. 158 (1978) 233.
[72] K.B. Sentell, J.G. Dorsey, Anal. Chem. 61 (1989) 930.
[73] K.B. Sentell, J.G. Dorsey, J. Chromatogr. 461 (1989) 193.
[74] K. Miyabe, G. Guiochon, J. Chromatogr. 166 (1978) 21.
[75] F. Gritti, G. Guiochon, J. Chromatogr. A 1115 (2006) 142.
[76] C. Horvath, W. Melander, I. Molnar, J. Chromatogr. 125 (1976) 129.
[77] H.J. Mockel, G. Welter, H. Meltzer, J. Chromatogr. 388 (1978) 285.
[78] M.M. Schantz, D.E. Martire, J. Chromatogr. 391 (1978) 35.
[79] H. Colin, A.M. Krstulovic, M.F. Gonnord, G. Guiochon, Z. Yun, P. Jandera, Chromatographia 17 (1983) 9.
[80] A. Tchapla, H. Colin, G. Guiochon, Anal. Chem. 56 (1984) 621.
[81] L.R. Snyder, J. Chromatogr. 179 (1979) 167.
[82] J. Chmielowiec, H. Sawatzky, J. Chromatogr. Sci. 17 (1979) 245.
[83] R.K. Gilpin, A.A. Squires, J. Chromatogr. Sci. 19 (1981) 195.
[84] P. Dufek, J. Chromatogr. 299 (1984) 109.
[85] E. Grushka, H. Colin, G. Guiochon, J. Chromatogr. 245 (1982) 325.
[86] H.J. Issaq, S.D. Fox, K. Lindsey, J.H. McConnell, D.E. Weiss, J. Liq. Chromatogr. 10 (1987) 49.
[87] A.M. Krstulovic, H. Colin, A. Tchapla, G. Guiochon, Chromatographia 117 (1989) 228.
[88] M. Borówko, S. Sokoł owski, O. Pizio, in: M. Borówko (Ed.), Computational Methods in Surface and Colloid Science, M. Dekker, New York, 2000, p. 167.